Ecological processes can synchronize marine population dynamics over continental scales

Tarik C. Gouhier[a,1], Frédéric Guichard[b], and Bruce A. Menge[a]

[a]Department of Zoology, Oregon State University, Corvallis, OR 97331; and [b]Department of Biology, McGill University, Montréal, QC, Canada H3A 1B1

Edited* by Simon A. Levin, Princeton University, Princeton, NJ, and approved April 2, 2010 (received for review December 17, 2009)

Determining the relative importance of local and regional processes for the distribution of population abundance is a fundamental but contentious issue in ecology. In marine systems, classical theory holds that the influence of demographic processes and dispersal is confined to local populations whereas the environment controls regional patterns of abundance. Here, we use spatial synchrony to compare the distribution of population abundance of the dominant mussel *Mytilus californianus* observed along the West Coast of the United States to that predicted by dynamical models undergoing different dispersal and environmental treatments to infer the relative influence of local and regional processes. We reveal synchronized fluctuations in the abundance of mussel populations across a whole continent despite limited larval dispersal and strong environmental forcing. We show that dispersal among neighboring populations interacts with local demographic processes to generate characteristic patterns of spatial synchrony that can govern the dynamic distribution of mussel abundance over 1,800 km of coastline. Our study emphasizes the importance of dispersal and local dynamics for the distribution of abundance at the continental scale. It further highlights potential limits to the use of "climate envelope" models for predicting the response of large-scale ecosystems to global climate change.

dispersal | environmental variability | metapopulation | synchrony | cross-scale interactions

Synchronized fluctuations in abundance among spatially segregated populations are common in nature and can be used to quantify and understand the distribution of abundance in space and time (1). Synchrony can be induced by local intrinsic processes such as dispersal among populations and strong interactions with mobile predators or regional extrinsic processes such as spatially correlated environmental variability (1). Although these processes are well known, identifying their relative contribution to patterns of synchrony remains a challenge (1). Recent work has shown that when the processes that contribute to synchrony can be studied in isolation, be it via natural barriers to dispersal among populations (2, 3) or experimental manipulation (4), synchrony patterns can be ascribed to their underlying cause. However, when intrinsic and extrinsic causes of synchrony co-occur, as is the case in most systems, assigning synchrony patterns to any specific causal process becomes onerous (1). Here, we show that in marine populations experiencing both intrinsic and extrinsic sources of synchrony, the shape of spatial synchrony patterns can be used to infer the cause of synchrony and explain the regional distribution of abundance.

Marine population theory has relied mostly on the environment to explain the regional (>1,000 km) dynamics of populations. This focus is motivated by the lengthy pelagic larval stage commonly found in marine organisms, during which the larvae can be transported over large distances by strong nearshore currents (5). The potential for large-scale transport, along with the difficulties associated with measuring larval dispersal, has prompted many studies to assume either completely closed (no exportation of larvae to other populations) or completely open (no coupling between larval production and recruitment) demography (5, 6, but see refs. 7, 8). This assumption, typically associated with equilibrium dynamics at the local scale, has emphasized the effect of large-scale heterogeneity in nearshore environmental conditions on recruitment (i.e., supply-side theory) to explain the regional dynamics of marine populations (6, 9). However, recent progress on the quantification of larval dispersal distance has motivated the relaxation of demographic openness in several marine species (10–12). In light of these recent developments, we relax the assumptions of demographic openness and local equilibrium dynamics and compare the distribution of population abundance, predicted by dynamical metapopulation models undergoing different dispersal and environmental treatments, to that of the dominant mussel *Mytilus californianus*, observed along the West Coast of the United States, to assess the relative importance of nearshore environmental heterogeneity and dispersal.

Results and Discussion

Role of the Environment in Natural Mussel Populations. We first focus on the role of environmental heterogeneity by quantifying the strength and the consistency of the relationship between nearshore environmental conditions and the abundance (% cover) of *M. californianus*. Although nearshore environmental conditions have a strong effect on patterns of recruitment (13, 14), that effect seems lost on the regional distribution of *M. californianus* cover (15) (Fig. 1*A*). Indeed, the spatial correlation between the environmental conditions and the mean annual *M. californianus* cover is relatively weak and inconsistent through time (Fig. 1*A*), regardless of the temporal lag used (Fig. S1), the temporal scale over which the environment is averaged (Fig. S2) or whether the analysis explicitly accounts for the spatial heterogeneity observed in nearshore conditions (Fig. S3). This weak spatial correlation reflects the mismatch between the persistent spatial gradient in the environment and the spatiotemporal variability in the cover of *M. californianus* (Fig. S3). This mismatch leads to local correlations whose strength and sign vary in space and time (Fig. S3). Once spatially averaged, these highly variable local correlations lead to weak and inconsistent spatial correlations at the regional scale (Fig. 1*A* and Fig. S2). Spatial synchrony, which measures the correlation in the time series of pairs of sites as a function of the lag distance that separates them (*Materials and Methods*), more succinctly reveals the same discrepancy between the persistent spatial gradient in nearshore environmental conditions and the more complex spatiotemporal patterns in the cover of *M. californianus* (Fig. 1*B*). All environmental variables undergo a slow and statistically significant linear decrease in synchrony with increasing lag distance (Fig. 1*B*, see *Materials and Methods* and Table 1 for statistical details). However, the cover of *M. californianus* shows a statistically significant nonlinear pattern,

Author contributions: T.C.G. and F.G. designed research; T.C.G. performed research; T.C.G. analyzed data; and T.C.G., F.G., and B.A.M. wrote the paper.

The authors declare no conflict of interest.

*This Direct Submission article had a prearranged editor.

[1]To whom correspondence should be addressed. E-mail: tarik.gouhier@gmail.com.

This article contains supporting information online at www.pnas.org/lookup/suppl/doi:10.1073/pnas.0914588107/-/DCSupplemental.

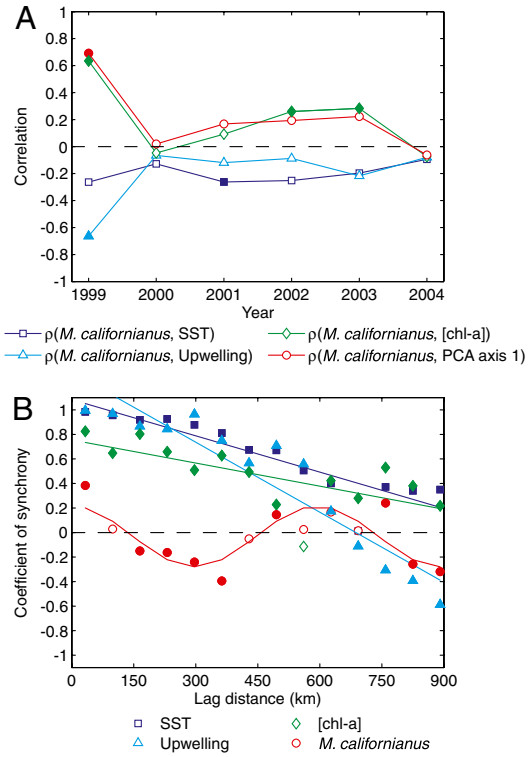

Fig. 1. The dynamics of *M. californianus* cover and the environment along the West Coast of the United States. (*A*) The correlation between the mean annual *M. californianus* cover and the 1-year lagged mean annual (*i*) sea surface temperature (SST, dark blue squares), (*ii*) chl-a concentration (chl-a, green diamonds), (*iii*) upwelling index (light blue triangles), and (*iv*) the first axis of the principal component analysis of all three environmental variables (PCA axis 1, red circles) at each site. (*B*) Spatial synchrony of the mean annual (*i*) *M. californianus* cover (red circles), SST (dark blue squares), chl-a (green diamonds), and upwelling index (light blue triangles). The curves correspond to nonlinear (*M. californianus*) and linear (chl-a, SST, and upwelling index) statistical models fitted to each data set (*Materials and Methods*). Full circles indicate statistical significance ($\alpha = 0.05$).

oscillating between synchrony and asynchrony with increasing lag distance (Fig. 1*B* and Table 1). This discrepancy suggests that intrinsic processes (i.e., dispersal and species interactions) rather than local nearshore environmental conditions may control the spatial synchrony patterns exhibited by *M. californianus*.

Effect of Dispersal and Species Interactions on Natural and Model Mussel Populations. To elucidate how dispersal and species interactions can generate the complex spatial synchrony patterns observed in natural *M. californianus* populations, we develop metapopulation models that describe disturbance–succession (16, 17) and predator–prey (18–20) dynamics in a network of mussel populations connected by dispersal. Dispersal was implemented as a symmetrical kernel in the successional model (*Materials and Methods*) and as a symmetrical and uniform nearest-neighbor process in the predator–prey model (*SI Text*). We subjected these metapopulation models to environmental variability treatments based on the nearshore environmental conditions observed along the West Coast of the United States by varying mussel fecundity (21) according to a linear spatial gradient (i.e., spatial environmental variability) and a linear spatial gradient with normally distributed white noise (i.e., spatiotemporal environmental variability; *Materials and Methods*). We now perform a factorial experiment on the metapopulation models by using different dispersal and environmental treatments to assess the relative importance of dispersal and environmental variability for generating nonlinear spatial synchrony patterns of abundance that are compatible with those observed in natural mussel populations.

When there is no dispersal (i.e., full local retention of larvae), regional mussel dynamics are strictly controlled by environmental heterogeneity. Under this scenario, the model metapopulations experiencing either spatial or spatiotemporal environmental variability predict a weak and inconsistent spatial correlation between the mussel cover and the 1-year lagged environmental conditions (Fig. 2 *A* and *B*). This weak and inconsistent relationship is compatible with the results from our survey data (Fig. 1*A*) and previously published accounts (15). However, model metapopulations predict that environmental variability induces a rapid decay in the spatial synchrony pattern of the mussel cover, which is incompatible with the nonlinear spatial synchrony pattern observed in natural populations of *M. californianus* (Fig. 2 *C* and *D*). We now introduce dispersal among populations and vary the environment and the scale of dispersal to determine their relative contribution to spatial synchrony.

When dispersal is limited to neighboring populations (herein "limited dispersal"; 8.6% of the spatial domain for results in Figs. 3 and 4), model metapopulations undergoing either spatial or spatiotemporal environmental variability predict a weak and inconsistent relationship between mussel cover and 1-year lagged environmental conditions (Fig. 3 *A* and *C*) that is similar to the one observed in the survey data (Fig. 1*A*). However, regional dispersal (44% of the spatial domain in Figs. 3 and 4) leads to a strong and dynamical relationship between the mussel cover and the environment (Fig. 3 *B* and *D*) that is inconsistent with the weak spatial correlation observed between populations of *M. californianus* and nearshore environmental conditions (Fig. 1*A*). This suggests that limited dispersal between fluctuating populations might be an important driver of abundance in natural populations of *M. californianus*. Indeed, this role of limited dispersal is made more evident through the analysis of spatial synchrony.

In metapopulations experiencing limited dispersal, both the successional model (Fig. 4 *A*, *C*, and *E*) and the predator–prey model (Fig. S4 *A*, *C*, and *E*) accurately predict the nonlinear spatial synchrony pattern observed in natural populations of *M. californianus*, regardless of environmental variability. In contrast, in metapopulations undergoing regional dispersal, both the successional model (Fig. 4 *B*, *D*, and *F*) and the predator–prey model (Fig. S4 *A*, *C*, and *E*) predict that the spatial synchrony pattern displayed by mussels will match the quasilinear decay displayed by the environment, despite the strong but inconsistent spatial correlation between the environment and mussel cover (Fig. 3 *B* and *D*). Hence, in successional and predator–prey metapopulation models, limited dispersal is critical for the emergence of nonlinear

Table 1. Fitting linear and nonlinear statistical models to the spatial synchrony patterns observed in the survey data sets

	Linear statistical model				Nonlinear statistical model			
Data set	*n*	*P* value	R^2	AIC_c	*n*	*P* value	R^2	AIC_c
chl-a	14	0.007	0.420	0.07	14	0.54	0.033	8.34
SST	14	8.6×10^{-6}	0.82	−10.48	14	0.77	0.007	13.36
Upwelling	14	7.3×10^{-7}	0.88	1.26	14	0.48	0.043	30.26
M. californianus	14	0.58	0.03	5.11	14	3.7×10^{-4}	0.67	−9.89

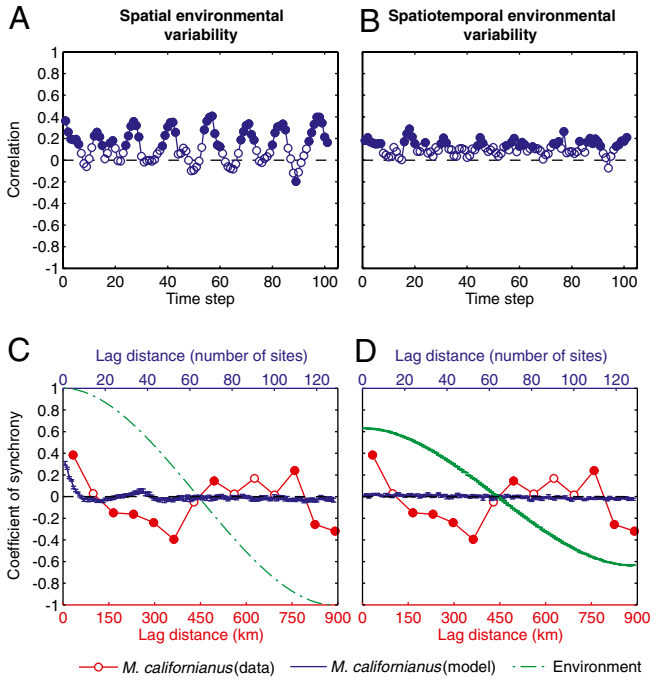

Fig. 2. The dynamics of the annual mussel cover in successional model metapopulations undergoing no dispersal and environmental variability. (*A* and *B*) The correlation between the model mussel cover and the 1-year lagged environment at each site during a randomly selected 100-time step window. (*C* and *D*) The coefficient of synchrony of the model (*i*) mussel cover (blue solid curve, mean ± SE) and the (*ii*) 1-year lagged environment (green dashed curve, mean ± SE). The spatial synchrony of the annual *M. californianus* cover from the West Coast of the United States is also depicted to facilitate comparisons (red circles). *A* and *C* correspond to spatial environmental variability whereas *B* and *D* correspond to spatiotemporal environmental variability. Full circles indicate statistical significance (α = 0.05).

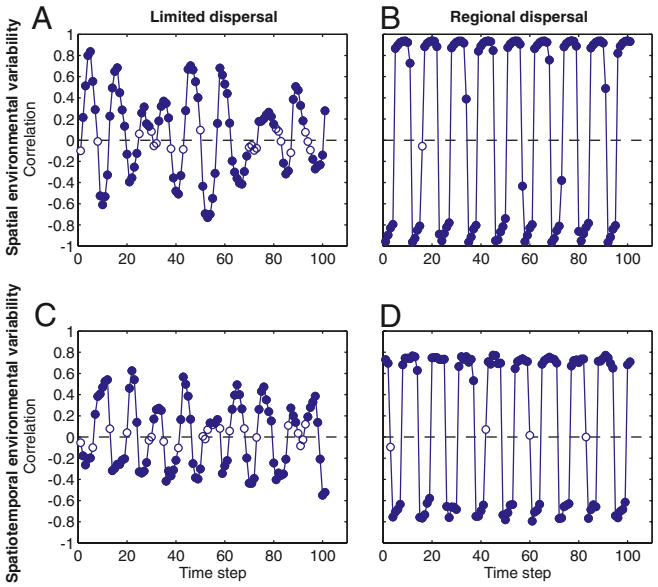

Fig. 3. Time series of the correlation between the annual mussel cover in the successional model and the 1-year lagged environment at each site. (*A* and *B*) The correlation time series for metapopulations undergoing spatial environmental variability and (*A*) limited (8.6% of the domain) or (*B*) regional (44% of the domain) dispersal. (*C* and *D*) Correlation time series for metapopulations undergoing spatiotemporal environmental variability and (*C*) limited or (*D*) regional dispersal. Full circles indicate statistical significance (α = 0.05).

spatial synchrony patterns that are compatible with those observed in natural populations of *M. californianus*. Nonlinear spatial synchrony patterns arise because limited dispersal (Fig. S5) couples neighboring populations and thus allows local fluctuations (Fig. S6) to scale up and generate complex, nonstationary spatiotemporal patterns at the regional scale (Figs. S7 and S8) that are robust to environmental forcing (Fig. 4 *B*, *D*, and *F* and Fig. S4 *B*, *D*, and *F*). This cross-scale interaction between local population dynamics and limited dispersal is a general property of metapopulations (Fig. 4 and Fig. S4) that merely requires that local populations undergo sustained fluctuations (Fig. S6) and that the average dispersal distance represents 3–10% of the spatial domain (Fig. S5). Regional dispersal prevents these cross-scale interactions by spatially synchronizing population fluctuations across the entire metapopulation and thus generating regular regional oscillations characterized by stationary and quasilinear spatial synchrony patterns (Fig. 4 *B*, *D*, and *F* and Figs. S4 *B*, *D*, and *F*, S9, and S10). The shape of spatial synchrony can thus be used to determine the relative influence of cross-scale interactions and environmental forcing on the distribution of abundance in space and time. This can be achieved by fitting nonlinear and linear statistical models representing, respectively, cross-scale interactions and environmental forcing to the observed spatial synchrony patterns and then comparing their performance using model selection (*Data Analysis* and Fig. S5).

Using Spatial Synchrony to Quantify the Scale of Dispersal in Natural Populations. Our metapopulation models show that the shape of nonlinear spatial synchrony patterns can be used to quantify the scale of dispersal. Indeed, the spatial range, defined as the lag distance at which synchrony first reaches zero (22), is systematically associated with the average dispersal distance in both our successional model (Fig. 4 *A*, *C*, and *E*) and our predator–prey model (Fig. S4 *A*, *C*, and *E*) when dispersal is limited. Applying this result to our survey data, we estimate that the scale of dispersal of *M. californianus* is ≈100 km (i.e., 6% of the domain). This estimate falls within the 95% confidence interval of dispersal distances documented for other bivalve species (72–220 km, see ref. 11) and is very similar to the scale of dispersal (97–115 km) of more closely related *Mytilus* species in other systems (11). Our estimate is based on the number of recruits that survive to the adult stage and is smaller than the 250-km estimate derived empirically by measuring the density of settlers in the same system (23). This is because spatial synchrony estimates integrate postsettlement processes that can limit the effective scale of dispersal.

Spatial Synchrony Reveals the Relative Influence of Intrinsic and Extrinsic Processes on the Distribution of Population Abundance. Theory has shown that local dynamics and limited dispersal can lead to complex spatial (24, 25) or spatiotemporal (26, 27) patterns at the regional scale that can promote coexistence (28), stability (27, 29), persistence (26, 29, 30), and functioning (24, 25) in spatial ecological systems. Similar complex spatiotemporal patterns have also been used to describe insect (31) and epidemic (32) outbreaks at regional and continental scales. However, linking local dynamics and limited dispersal to regional patterns has typically required extensive time series and characteristic spatial signatures such as Turing structures (24, 25), traveling waves (26, 31), or power laws (33). Here, we extend these theories by showing that in systems lacking these characteristic spatial signatures, the shape of spatial synchrony patterns can be used to infer the joint effect of local dynamics and dispersal on the regional distribution of abundance. Hence, our framework moves away from the use of correlations between abundance and the environment to infer the causal effect of abiotic processes on biological patterns. Instead, by partitioning

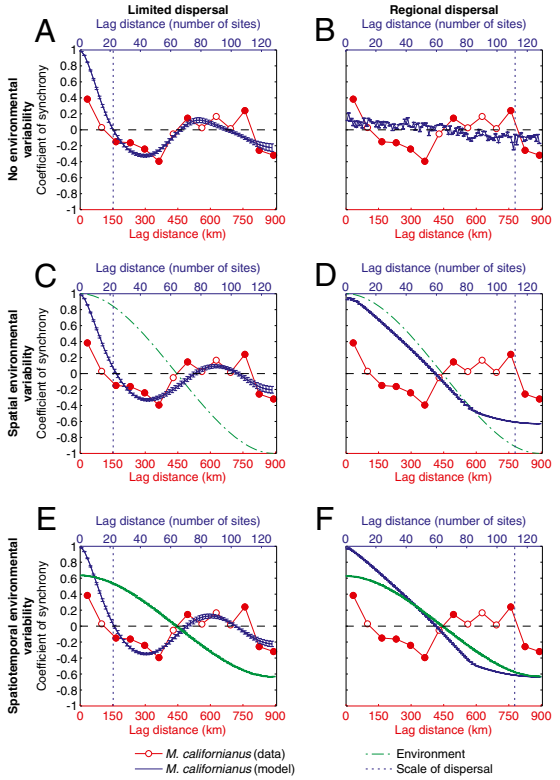

Fig. 4. Spatial synchrony of annual mussel cover in the successional model for metapopulations undergoing different environmental and dispersal treatments. (*A* and *B*) No environmental variability and either (*A*) limited or (*B*) regional dispersal. (*C* and *D*) Spatial environmental variability and either (*C*) limited or (*D*) regional dispersal. (*E* and *F*) Spatiotemporal environmental variability and either (*E*) limited or (*F*) regional dispersal. The spatial synchrony of the mussel cover in the successional model is represented in blue solid curves (mean ± SE), whereas that of the 1-year lagged environment is represented in green dashed curves (mean ± SE). The spatial synchrony of annual *M. californianus* cover from the West Coast of the United States is also depicted to facilitate comparisons (red circles). The scale of dispersal is represented by the blue vertical dotted line. The spatial extent of the limited dispersal treatment corresponds to 8.6% of the domain, whereas that of the regional dispersal treatment corresponds to 44% of the domain. Full circles indicate statistical significance ($\alpha = 0.05$).

long nonstationary time series into smaller quasistationary time series and applying spatial synchrony analysis, we show that the spatial and temporal properties of spatial synchrony patterns can be used to determine the relative influence of intrinsic and extrinsic factors on the regional distribution of abundance in natural systems: limited dispersal interacts with local intrinsic fluctuations to generate nonlinear and nonstationary spatial synchrony patterns that are robust to environmental forcing, whereas regional dispersal facilitates environmental forcing and leads to stationary and linear spatial synchrony patterns.

Our results have important implications for identifying the processes that control the distribution of species abundance in natural systems and for predicting their response to global climate change. A popular approach for understanding and predicting species abundance distributions is to build species' "climate envelopes" by either mapping the current species distribution to climate variables via correlation techniques or by determining the physiological tolerances of individual species (see review in ref. 34). This climate envelope can then be used to predict the future distribution of species under various climate change scenarios (34). However, climate envelope models have been criticized because they do not integrate the effects of species interactions and dispersal on the distribution of population abundance (35–38). A recent synthesis proposes integrating the effects of dispersal and species interactions into climate envelopes by adopting a hierarchical modeling framework (34). According to this hierarchical framework, species interactions and dispersal control the distribution of species abundance at smaller spatial scales (<200 km) whereas climate dominates at larger spatial scales (>200 km) (34). Here, we have shown that despite strong regional environmental forcing, local dynamics interact with limited dispersal to control the distribution of population abundance at scales that are much larger (>1,000 km) than that of dispersal (~100 km). Hence, our work suggests that processes occurring at small spatial scales can interact synergistically to control the distribution of population abundance at large spatial scales. Such cross-scale interactions demonstrate the limitations of adopting climate envelope models based on hierarchical frameworks to understand the distribution of species abundance and predict the effects of global climate change.

Overall, by applying spatial synchrony analysis to a large data set of mussel populations along the West Coast of the United States, our study provides unique evidence that limited connectivity among local populations affects the dynamic distribution of abundance over >1,000 km. Our work supports the suggested shift toward a more dynamical approach to regional conservation, one that emphasizes patterns and processes across scales instead of those limited to the scale of the environment or dispersal.

Materials and Methods

Data Collection. Abundance (percent cover) of *M. californianus* was quantified annually from 1999 to 2004 at 48 sites located along the West Coast of the United States and stretching from southern California to northern Washington (39) (32.7 °N to 48.4 °N). For each site, the cover of *M. californianus* was surveyed in 10 randomly placed 0.25 m^2 quadrats for each of three 50-m transects located within the midintertidal zone. Mean annual sea surface temperature (SST, in °C), chlorophyll-a concentration (chl-a, in mg/m^3), and upwelling index (in m^3/s/100 m of coastline) data from 1997 to 2003 occurring within a 0.2 degree radius (1 degree radius for upwelling) of each of the 48 sites were obtained, respectively, from the advanced very high resolution radiometer (NOAA), the sea-viewing wide field-of-view sensor (NASA), and sea level pressure maps (Pacific Fisheries Environmental Laboratory). These environmental data series were validated by comparing them to in situ buoy measurements (see *Data Validation* in *SI Text*).

Data Analysis. Before conducting spatial synchrony analysis, all variables were detrended by subtracting the global mean time series from each site's time series to remove any bias caused by common large-scale trends (40). The distances between all pairs of sites were then computed and used to group the detrended time series data into equally spaced distance bins (66 km wide). The coefficient of synchrony for each bin was calculated by computing the correlation coefficient between the time series of all pairs of sites within the bin. The extent of the spatial synchrony analysis was restricted to half of the spatial domain to avoid large discrepancies in the number of pairs of sites within each bin (22). Statistical significance was determined by using a one-tailed test ($\alpha = 0.05$) on 10,000 Monte Carlo randomizations (22). Specifically, for each bin, the *P* value was calculated by shuffling the data pairs within the bin 10,000 times, computing the coefficient of synchrony for each randomization, and then calculating the proportion of randomizations with a coefficient of synchrony greater than or equal to that obtained with the original data. The same one-tailed randomization technique was used to assess the statistical significance of the correlation between the annual cover of *M. californianus* at year *i* and each environmental variable at year *i-1* (1-year lag). We used a 1-year lag because it corresponds to the temporal scale at which the correlation between the annual cover of *M. californianus* and each nearshore environmental variable is statistically significant (Fig. S1).

We used model selection to detect linear and nonlinear spatial synchrony patterns in the environmental (SST, chl-a, and upwelling index) and *M. californianus* data sets. For each data set, we fit a linear statistical model $m|_{\text{linear}}$ and a nonlinear statistical model $m|_{\text{nonlinear}}$ to the spatial synchrony pattern:

$$m|_{\text{linear}} = a \cdot l + b \qquad [1]$$

$$m|_{\text{nonlinear}} = a \cdot \cos\left(\frac{l}{\max(l)} \cdot 3\pi\right) + b, \qquad [2]$$

where l is the lag distance vector, a,b represent fitted coefficients and $\frac{l}{\max(l)} \cdot 3\pi$ is the normalized lag distance vector scaled to the domain $[0, 3\pi]$. This scaling of the lag distance vector allows the cosine function in the nonlinear model $m|_{\text{nonlinear}}$ to fit modal patterns of spatial synchrony over the spatial domain. For each statistical model, we calculated the Akaike information criterion corrected for small samples (41):

$$\text{AIC}_c = -2\log(L) + 2K + \frac{2K(K+1)}{n-K-1}, \qquad [3]$$

where L represents the maximum likelihood, $K = 3$ represents the number of parameters in each statistical model, and n represents the number of samples. The statistical model with the smallest AIC_c value was selected for each data set (41).

Successional Model. The successional model describes local disturbance and recovery dynamics in a network of mussel populations that are connected by dispersal (17). Within populations, the successional dynamics observed in natural intertidal systems (16, 42) are represented as a mean-field implementation of a spatial process affecting the proportional abundance of (*i*) the dominant mussel (m), (*ii*) the wave disturbance (w), and (*iii*) the empty substrate (s) (43). A maximum fraction $\alpha_0 = 1$ of the proportional abundance of the dominant mussel species (m) can be displaced by wave disturbances (w). A proportion $(1-\delta_0)$ of disturbances displaces mussels through a density-dependent contact process with aggregation (Moore neighborhood, $q = 8$), whereas a proportion $\delta_0 = 10^{-3}$ of disturbances is density independent. This disturbance dynamic is based on the assumption that wave disturbances destroy the byssal thread attachments of mussels around the edges of disturbed areas, thus making them temporarily more susceptible to further disturbance (43, 44). Hence, newly disturbed areas allow the local propagation of wave disturbances to adjacent mussel beds. Once the disturbance has propagated away from the newly disturbed area, the area transitions from the "wave disturbed" state to the "empty substrate" state. Similarly to disturbance, a maximum fraction $\alpha_2 = 0.65$ of the empty substrate (s) can be colonized by mussels. A proportion $\delta_2 = 0.1$ of colonization occurs through a density-independent process, whereas the remaining colonization is density dependent $(1-\delta_2)$. Mussel colonization also depends on the production and recruitment of larvae. Within populations x, larval production is a function of local mussel proportional abundance m_x and fecundity f_x $(\bar{f} = 5.25)$. The recruitment rate C_x^t is described by a Poisson process (45) $C_x^t = 1 - e^{-\beta_x^t}$, where β_x^t integrates (*i*) the total number of larvae produced and retained in populations x at time t and (*ii*) the total number of larvae produced in other populations y and dispersed to populations x at time t. The dynamics of the model are represented by the following integro-difference equation system for populations x in a metapopulation consisting of $n = 256$ populations:

$$\begin{aligned} w_x^{t+1} &= \alpha_0 m_x^t\left(\delta_0 + (1-\delta_0)\left(1-\left(1-w_x^t\right)^q\right)\right) \\ s_x^{t+1} &= w_x^t + s_x^t - \alpha_2 C_x^t s_x^t\left(\delta_2 + m_x^t(1-\delta_2)\right) \\ m_x^{t+1} &= 1 - w_x^t - s_x^t \end{aligned} \qquad [4]$$

with:

$$\begin{aligned} C_x^t &= 1 - e^{\beta_x^t} \\ \beta_x^t &= m_x^t f_x (1-d) + \int m_y^t f_y dD(|x-y|)\mathrm{d}y \\ D(|x-y|) &= \tfrac{3|x-y|^2}{2} e^{-|x-y|^3} \\ x &= u\left(\tfrac{2}{n}\mathbf{L} - 1\right) \\ \mathbf{L} &= \begin{bmatrix} 0 \\ \vdots \\ n-1 \end{bmatrix} \end{aligned}, \qquad [5]$$

where D is the symmetrical mussel dispersal kernel resulting from larval transport at a constant speed and with a time-dependent settlement rate (double Weibull distribution) (46), d represents the proportion of larvae being dispersed, u represents the scale of dispersal, and $\mathbf{L}$ represents a zero-based vector of population locations. We vary dispersal by manipulating d, the proportion of larvae being dispersed ($d = 0$ means that all larvae are retained locally, whereas $d = 1$ means that all larvae are dispersed), and u, the scale of dispersal ($u = 2$ corresponds to regional dispersal and $u = 10$ corresponds to limited dispersal). We assumed periodic boundary conditions for all simulations and set the dispersal rate to $d = 1$ (i.e., no local retention) unless otherwise specified (i.e., Fig. 2 where $d = 0$). All successional model simulations were performed for 256 populations and the results were analyzed over 2,000 posttransient time steps. Because our goal was to test the importance of local ecological processes and dispersal, all parameter values detailed above were selected to be representative of the broad parameter space characterized by spatiotemporal heterogeneity (17, 47). Here, we further assess the model's sensitivity to dispersal distance and to fecundity f as a means to determine the role of environmental variability in marine metapopulations.

Environmental variability can have a significant impact on the productivity of intertidal populations (21, 48). Here, we implement this effect by varying mussel fecundity spatially and spatiotemporally. Specifically, the spatial environmental treatment consists of varying the mussel fecundity f linearly from 3 to 7.5 over the entire spatial range $(\bar{f} = 5.25)$. We generate the spatiotemporal environmental treatment by adding normally distributed white noise with zero mean and variance $\sigma^2 = 2.7$ to the previously described spatial variation in fecundity $(\bar{f} = 5.25)$. The spatial and spatiotemporal environmental treatments thus preserve the same mean fecundity as the successional model undergoing no environmental variability. These spatial and spatiotemporal treatments were chosen to roughly mimic the spatial and spatiotemporal properties of the environment along the West Coast of the United States. Applying the same spatial and spatiotemporal treatments to the mussel growth rate α_2 yields qualitatively similar results.

Model Analysis. We applied the spatial synchrony and model selection methods (*Data Analysis*) used on the survey data to the posttransient time series of the successional and the predator–prey (*SI Text*) models to assess their ability to generate nonlinear spatial synchrony patterns that are compatible with those observed in natural populations of *M. californianus*. Specifically, the model time series (2,000 posttransient time steps) was split into 10-time step windows and spatial synchrony analysis was conducted over each window. We chose 10-time step windows to approximate the temporal extent of our intertidal survey data. However, our results are robust to window size (Fig. S5 *B*, *D*, and *F*). For each time window, we fit the same linear $(m|_{\text{linear}})$ and nonlinear $(m|_{\text{nonlinear}})$ statistical models described in *Data Analysis* to the spatial synchrony patterns generated by the metapopulation models. For each time window, the nonlinear statistical model was selected if $\text{AIC}_c|_{\text{nonlinear}} < \text{AIC}_c|_{\text{linear}}$ (41). The model spatial synchrony patterns presented in all figures were computed by averaging the spatial synchrony patterns from all 10-time step windows in which the nonlinear statistical model was selected. When no compatible synchrony pattern exists for the entire model time series (i.e., for the regional dispersal treatment), the spatial synchrony patterns from n randomly selected time windows are computed and averaged (where n corresponds to the number of compatible synchrony patterns for the limited dispersal treatment). This allows for unbiased comparisons across dispersal treatments.

ACKNOWLEDGMENTS. We thank G. Fussmann, B. Cazelles, and J. van de Koppel for providing insightful comments on a previous version of the manuscript. T.C.G. was supported by a McGill Majors fellowship; F.G. was supported by a grant from the James S. McDonnell Foundation; B.A.M was supported by grants from the David and Lucile Packard Foundation, the Gordon and Betty Moore Foundation, the Wayne and Gladys Valley Foundation, the Andrew W. Mellon Foundation, and the National Science Foundation. This is publication number 360 from the Partnership for Interdisciplinary Studies of Coastal Oceans (PISCO), a large-scale, long-term consortium primarily funded by the David and Lucile Packard Foundation and the Gordon and Betty Moore Foundation.

1. Liebhold A, Koenig WD, Bjornstad ON (2004) Spatial synchrony in population dynamics. *Annu Rev Ecol Evol Syst* 35:467–490.
2. Post E, Forchhammer MC (2002) Synchronization of animal population dynamics by large-scale climate. *Nature* 420:168–171.
3. Grenfell BT, et al. (1998) Noise and determinism in synchronized sheep dynamics. *Nature* 394:674–677.
4. Vasseur DA, Fox JW (2009) Phase-locking and environmental fluctuations generate synchrony in a predator-prey community. *Nature* 460:1007–1010.
5. Roughgarden J, Iwasa Y, Baxter C (1985) Demographic theory for an open marine population with space-limited recruitment. *Ecology* 66:54–67.
6. Connolly SR, Roughgarden J (1999) Theory of marine communities: Competition, predation, and recruitment-dependent interaction strength. *Ecol Monogr* 69:277–296.

7. Hastings A, Higgins K (1994) Persistence of transients in spatially structured ecological models. *Science* 263:1133–1136.
8. Alexander SE, Roughgarden J (1996) Larval transport and population dynamics of intertidal barnacles: A coupled benthic/oceanic model. *Ecol Monogr* 66:259–275.
9. Roughgarden J, Gaines SD, Pacala SW (1987) *Supply-Side Ecology: The Role of Physical Transport Processes* (Blackwell Scientific Publications, London), pp 491–495.
10. Swearer SE, et al. (2002) Evidence of self-recruitment in demersal marine populations. *Bull Mar Sci* 70:251–271.
11. Kinlan BP, Gaines SD (2003) Propagule dispersal in marine and terrestrial environments: A community perspective. *Ecology* 84:2007–2020.
12. Gilg MR, Hilbish TJ (2003) The geography of marine larval dispersal: Coupling genetics with fine-scale physical oceanography. *Ecology* 84:2989–2998.
13. Connolly SR, Menge BA, Roughgarden J (2001) A latitudinal gradient in recruitment of intertidal invertebrates in the northeast Pacific Ocean. *Ecology* 82:1799–1813.
14. Connolly SR, Roughgarden J (1998) A latitudinal gradient in northeast Pacific intertidal community structure: Evidence for an oceanographically based synthesis of marine community theory. *Am Nat* 151:311–326.
15. Menge BA, Chan F, Nielsen KJ, Lorenzo ED, Lubchenco J (2009) Climatic variation alters supply-side ecology: Impact of climate patterns on phytoplankton and mussel recruitment. *Ecol Monogr* 79:379–395.
16. Paine RT, Levin SA (1981) Inter-tidal landscapes: Disturbance and the dynamics of pattern. *Ecol Monogr* 51:145–178.
17. Guichard F (2005) Interaction strength and extinction risk in a metacommunity. *Proc R Soc Lond B Biol Sci* 272:1571–1576.
18. Paine RT (1966) Food web complexity and species diversity. *Am Nat* 100:65–75.
19. Rosenzweig ML, MacArthur RH (1963) Graphical representation and stability conditions of predator-prey interactions. *Am Nat* 97:209–223.
20. Holland MD, Hastings A (2008) Strong effect of dispersal network structure on ecological dynamics. *Nature* 456:792–794.
21. Leslie HM, Breck EN, Chan F, Lubchenco J, Menge BA (2005) Barnacle reproductive hotspots linked to nearshore ocean conditions. *Proc Natl Acad Sci USA* 102: 10534–10539.
22. Fortin M, Dale M (2005) *Spatial Analysis: A Guide for Ecologists* (Cambridge Univ Press, Cambridge, UK).
23. Navarrete SA, Broitman BR, Menge BA (2008) Interhemispheric comparison of recruitment to intertidal communities: Pattern persistence and scales of variation. *Ecology* 89:1308–1322.
24. Rietkerk M, van de Koppel J (2008) Regular pattern formation in real ecosystems. *Trends Ecol Evol* 23:169–175.
25. van de Koppel J, et al. (2008) Experimental evidence for spatial self-organization and its emergent effects in mussel bed ecosystems. *Science* 322:739–742.
26. Blasius B, Huppert A, Stone L (1999) Complex dynamics and phase synchronization in spatially extended ecological systems. *Nature* 399:354–359.
27. Jansen V, de Roos A (2000) The role of space in reducing predator-prey cycles. *The Geometry of Ecological Interactions: Simplifying Spatial Complexity*, eds Dieckmann U, Law R, Metz JAJ (Cambridge Univ Press, Cambridge, UK), pp 183–201.
28. Hassell MP, Comins HN, May RM (1994) Species coexistence and self-organizing spatial dynamics. *Nature* 370:290–292.
29. Briggs CJ, Hoopes MF (2004) Stabilizing effects in spatial parasitoid-host and predator-prey models: A review. *Theor Popul Biol* 65:299–315.
30. Hassell MP, Comins HN, May RM (1991) Spatial structure and chaos in insect population dynamics. *Science* 353:255–258.
31. Bjornstad ON, Peltonen M, Liebhold AM, Baltensweiler W (2002) Waves of larch budmoth outbreaks in the European Alps. *Science* 298:1020–1023.
32. Viboud C, et al. (2006) Synchrony, waves, and spatial hierarchies in the spread of influenza. *Science* 312:447–451.
33. Solé R, Bascompte J (2006) *Self-Organization in Complex Ecosystems.* (Princeton Univ Press, Princeton).
34. Pearson RG, Dawson TP (2003) Predicting the impacts of climate change on the distribution of species: Are bioclimate envelope models useful? *Glob Ecol Biogeogr* 12:361–371.
35. Suttle KB, Thomsen MA, Power ME (2007) Species interactions reverse grassland responses to changing climate. *Science* 315:640–642.
36. Gill JA, et al. (2001) The buffer effect and large-scale population regulation in migratory birds. *Nature* 412:436–438.
37. Davis AJ, Jenkinson LS, Lawton JH, Shorrocks B, Wood S (1998) Making mistakes when predicting shifts in species range in response to global warming. *Nature* 391:783–786.
38. Davis AJ, Lawton JH, Shorrocks B, Jenkinson LS (1998) Individualistic species responses invalidate simple physiological models of community dynamics under global environmental change. *J Anim Ecol* 67:600–612.
39. Schoch GC, et al. (2006) Fifteen degrees of separation: Latitudinal gradients of rocky intertidal biota along the California current. *Limnol Oceanogr* 51:2564–2585.
40. Koenig WD (1999) Spatial autocorrelation of ecological phenomena. *Trends Ecol Evol* 14:22–26.
41. Burnham K, Anderson D (2002) *Model Selection and Multimodel Inference: A Practical Information-Theoretic Approach* (Springer, New York).
42. Paine RT (1984) Ecological determinism in the competition for space. *Ecology* 65: 1339–1348.
43. Guichard F, Halpin PM, Allison GW, Lubchenco J, Menge BA (2003) Mussel disturbance dynamics: Signatures of oceanographic forcing from local interactions. *Am Nat* 161: 889–904.
44. Denny MW (1987) Lift as a mechanism of patch initiation in mussel beds. *J Exp Mar Biol Ecol* 113:231–245.
45. Caswell H, Etter R (1999) Cellular automaton models for competition in patchy environments: Facilitation, inhibition, and tolerance. *Bull Math Biol* 61:625–649.
46. Neubert MG, Kot M, Lewis MA (1995) Dispersal and pattern-formation in a discrete-time predator-prey model. *Theor Popul Biol* 48:7–43.
47. Guichard F, Steenweg R (2008) Intrinsic and extrinsic causes of spatial variability across scales in a metacommunity. *J Theor Biol* 250:113–124.
48. Menge BA, Daley BA, Wheeler PA, Strub PT (1997) Rocky intertidal oceanography: An association between community structure and nearshore phytoplankton concentration. *Limnol Oceanogr* 42:57–66.